Nuclear Physics A 674 (2000) 29–46

NUCLEAR PHYSICS A

www.elsevier.nl/locate/npe

The GDR width in the excited ^{147}Eu compound nucleus at high angular momentum

M. Kmiecik [a], A. Maj [a,*], A. Bracco [b], F. Camera [b], M. Casanova [b], S. Leoni [b], B. Million [b], B. Herskind [c], R.A. Bark [c,1], W.E. Ormand [d]

[a] *The Niewodniczański Institute of Nuclear Physics, ul. Radzikowskiego 152, PL-31-342 Krakow, Poland*
[b] *Dipartimento di Fisica, Universita di Milano and INFN sez. Milano, I-20133 Milano, Italy*
[c] *The Niels Bohr Institute, University of Copenhagen, DK-2100 Copenhagen, Denmark*
[d] *Physics Directorate, Lawrence Livermore National Laboratory, L-414, P.O. Box 808, Livermore, CA 94551, USA*

Received 16 December 1999; revised 21 February 2000; accepted 2 March 2000

Abstract

High-energy γ-rays emitted in the decay of the hot compound nucleus ^{147}Eu have been measured in coincidence with low-energy γ-rays. The γ transitions from the different residual nuclei were detected by a multiplicity filter and by Ge detectors. The employed reaction was $^{37}\mathrm{Cl} + {}^{110}\mathrm{Pd}$ at bombarding energies of 160, 165 and 170 MeV. The measured high-energy γ-ray spectra were analysed within the framework of the statistical model using the CASCADE code. The GDR width in the angular momentum interval between 35 and 50 $\hbar$ was found to increase weakly and to be rather well predicted by the thermal shape fluctuation model. Also the deformation parameter β as a function of the average angular momentum extracted from the data was found to be in general agreement with the model. © 2000 Elsevier Science B.V. All rights reserved.

PACS: 21.10.Re; 24.30.Cz; 25.70.Gh
Keywords: NUCLEAR REACTIONS $^{110}\mathrm{Pd}(^{37}\mathrm{Cl}, x\mathrm{n})$; $E = 160, 165, 170$ MeV; Measured E_γ, I_γ of high- and low-energy γ-rays; γ-multiplicity; ^{147}Eu compound nucleus; γ-decay of GDR; GDR width; Deformation parameters; CASCADE calculations; Thermal shape fluctuations

1. Introduction

During the last several years, a systematic effort has been made to investigate the properties of the giant dipole resonance built on excited states. These investigations indicate that the resonance becomes broader as a function of excitation energy. In particular, the

* Corresponding author: E-mail: adam.maj@ifj.edu.pl; tel.: +(4812)-6370222; fax: +(4812)-6371881
[1] Present address: Department of Nuclear Physics, R.S. Phys. S.E., Australian National University, Canberra, ACT 0200, Australia.

0375-9474/00/$ – see front matter © 2000 Elsevier Science B.V. All rights reserved.
PII: S0375-9474(00)00166-4

temperature effects of the two main damping mechanisms responsible for the observed GDR width, namely collisional damping and thermal shape fluctuations have been studied by several authors [1,2]. The most convincing picture concerning this problem obtained so far, by comparing data with predictions, is that collisional damping is basically independent of temperature (at least up to 2 MeV) and that the coupling to the quadrupole nuclear deformation together with the effects of thermal shape fluctuation is responsible for the width increase. In fact, in the case of nuclei in the mass region $A \approx 110$, thermal shape fluctuation calculations using as intrinsic width (collisional damping width) the $T = 0$ values, can in general reproduce the temperature dependence of the width at very small and constant angular momentum as well as the angular momentum dependence at almost constant temperature [3–5]. It is clear from what we have learned so far in connection with the important role of the nuclear shape in the GDR width that one needs to test the model of thermal shape fluctuations in different situations. In fact, one expects that the average nuclear shape can change due to both temperature and angular momentum effects. It is therefore very important to have selective data in which one of the two quantities (temperature or angular momentum) is basically fixed to be compared with predictions. In particular, the study of shape effects induced by angular momentum data at high spins can provide a stringent test of the model because the largest deformations are expected in this case.

The comparison of the results for the GDR width in ^{106}Sn and ^{176}W at high angular momentum ($I > 35\ \hbar$), has shown that the angular momentum effects depend on the nuclear moment of inertia. In fact, while the measured GDR width of medium heavy nuclei $^{106-110}$Sn strongly depends on the angular momentum, in the more heavy nucleus ^{176}W it is almost spin independent. This last point has been also confirmed by a more recent measurement on the Hg isotopes sampling in this case the angular momentum interval 20–36 $\hbar$ [6]. For a nucleus with a mass such as $A \approx 150$ and between that of Sn and W one expects an intermediate behaviour.

The present paper reports a measurement of γ-decay from the giant dipole resonance built on the excited ^{147}Eu nucleus in the angular momentum interval 35–50 $\hbar$. The ^{147}Eu nucleus is particularly interesting, not only to test the thermal shape fluctuation model in this mass region but also for another reason. Namely the ^{143}Eu residual nucleus at high angular momenta has shown some evidence for the existence at a few MeV above the yrast line of the GDR built on superdeformed configurations [7–9]. A natural question is therefore whether or not one can find a trace of this superdeformation also in the value of GDR width which is deduced from more inclusive data. This is an important point because if no evidence of superdeformation is seen in the more inclusive data one can have a further confirmation that superdeformation is a property of the rather cold nucleus and can also have more confidence on the pure statistical description of high energy γ-ray emission.

In the experiment both high and low-energy γ-rays were detected. By measuring low-energy γ-rays, the population yields of the different residual nuclei were obtained as a function of angular momentum. This additional information, which is not usually obtained in more standard GDR experiments, improves the quality of the statistical model analysis of the high-energy γ-ray spectra. In fact, to deduce the values of the GDR parameters from the measured high-energy spectra one has to rely on the appropriate choice of a number of other parameters, such as spin distribution, level density and yrast line which enter in the statistical model calculations. By measuring simultaneously other quantities in the same experiment, for example the residual distributions, one can therefore not only verify these choices, but also confirm the statistical nature of the γ-ray emission on which the study of the GDR parameters is based.

In the following two sections we describe the experiments and the data analysis procedure. In Section 4, the comparison with the prediction of the thermal shape fluctuation model is presented and discussed. A special emphasis is given to the discussion of the effective nuclear shape.

2. The experimental method

The experiment was performed at the Tandem Accelerator Laboratory of the Niels Bohr Institute. A 1.06 $\mathrm{mg/cm^2}$ target of ^{110}Pd, consisting of a sandwich of two layers 0.51 and 0.55 $\mathrm{mg/cm^2}$ thick enriched to 97.7%, was bombarded by a beam of ^{37}Cl produced by the Tandem+Booster accelerator system. Three beam energies 160, 165 and 170 MeV were employed forming the ^{147}Eu compound nucleus at excitation energy of 74, 78 and 81 MeV, respectively. The corresponding maximum angular momentum was 58, 62 and 64.5 $\hbar$, respectively, as deduced with the model of Winther [10]. The detection system used was the detector array HECTOR coupled to the NORDBALL detector system. With this apparatus, it was possible to measure the energy and time of high-energy γ-rays, the multiplicity and sum energy of low-energy γ-transitions, and the time and energy of γ-ray transitions in different residual nuclei. The HECTOR array [11] consists of 8 large volume BaF_2 crystals, one positioned at 0°, two at 37°, three at 60° and two at 79°. The NORDBALL array [12, 13] consisted of 17 Compton suppressed HPGe detectors and of an innerball of BaF_2 scintillators covering a solid angle of $\approx 2\pi$ used as a multiplicity filter. The separation between neutron and γ events was achieved by the time of flight measurement. Gain shifts of the photomultiplier tubes of large BaF_2 detectors were monitored with accuracy better than 0.2% using the LED system optically coupled to the crystals by optic fibers, and corrected off-line as necessary. The energy calibration of the high-energy detectors was done using the 15.1 MeV γ-rays from $\mathrm{D}(^{11}\mathrm{B}, \mathrm{n}\gamma)^{12}\mathrm{C}^*$ reaction as a high energy point and utilizing the feature of the SILENA 4418/Q ADC that any non-zero DC level, even if associated with the signal source, is traced and accurately cancelled.

The response function of the multiplicity filter was determined by making use of the method described in Ref. [11]. A total efficiency of 35% was measured for the 1.172 MeV line from a ^{60}Co source. The collected events were coincidences of high-energy gamma rays ($E_\gamma > 3$ MeV) measured in the BaF_2 detectors and γ-rays detected in HPGe and the multiplicity filter.

3. Experimental data analysis

The high-energy γ-ray data collected in the experiment were sorted into three different classes corresponding to the fold intervals 5–7, 5–30 and 8–30.

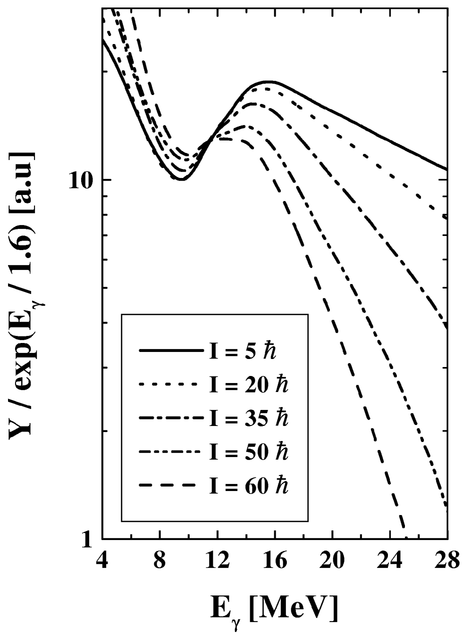

Fig. 1. Examples of γ-spectra calculated with CASCADE for the same GDR parameters, but for different values of the compound nucleus spin, divided by exponential function in order to enhance the GDR part. One can see that the apparent GDR centroid moves with spin.

The measured γ-ray spectra associated with the selected fold intervals were fit in the GDR region, namely from 8 to 18 MeV, with a modified version of the statistical model code CASCADE [14] using the Reisdorff approach for the level density [15–17]. The calculations were corrected for the detection response. The centroid and the width values were obtained from the best fit to the data using a χ^2 minimisation procedure.

One of the important quantities entering in the statistical model calculations and affecting the analysis of the high energy γ-ray spectra is the spin distribution of the compound nucleus. To illustrate the effect of angular momentum on the spectral shape of the high-energy γ-ray spectrum several calculated spectra corresponding to different spin, with the same GDR parameters, are shown in Fig. 1. The calculated spectra are divided by the same exponential function. As one can see the apparent centroid moves towards lower energy with increasing spin, and the distribution becomes narrower. It is therefore clear that the calculations associated with a selected fold interval need the best possible modelling of the corresponding spin distribution.

In the present case, the conversion from the measured fold (number of measured γ-rays) to the γ-multiplicity (number of γ-rays emitted in the reaction) was based on the method described in [11]. After that the spin distribution was constructed from the multiplicity distribution assuming the simple relation between spin J and multiplicity M: $J = 2M - S + I$, where S is the angular momentum removed by statistical γ-rays and I is a correction for the spin of isomers. The spin distributions corresponding to the folds 5–7, folds 8–30 and folds 5–30 regions are shown in the upper part of Fig. 2. In constructing these

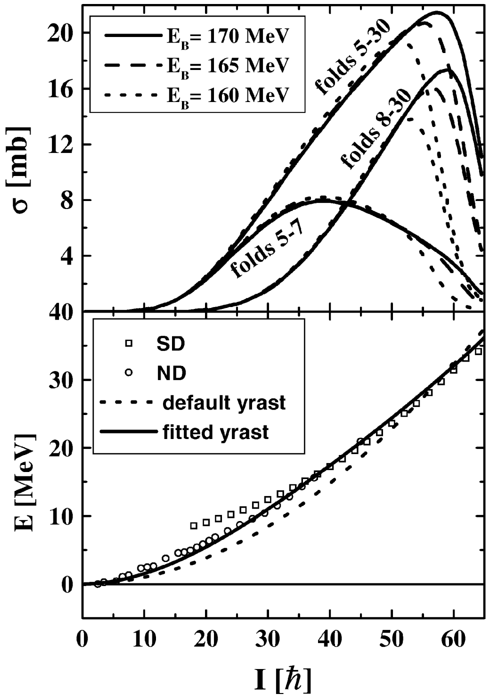

Fig. 2. Angular momentum distributions, corresponding to the different gating conditions, used as input in the CASCADE code. Bottom panel: yrast line (solid line) used as input in CASCADE calculations obtained form the fit to experimental data (normal: circles; superdeformed: squares). The CASCADE default yrast line (dashed line) is also indicated.

Table 1
Reaction parameters

		Fold 5–7	Fold 5–30	Fold 8–30
170 MeV Cl on Pd				
$E^* = 81.4$ MeV	$\langle I \rangle$ [$\hbar$]	39	45	50
$L_{\max} = 64.5\ \hbar$	$\langle T \rangle$	1.36	1.31	1.28
165 MeV Cl on Pd				
$E^* = 77.6$ MeV	$\langle I \rangle$ [$\hbar$]	38	44	49
$L_{\max} = 62\ \hbar$	$\langle T \rangle$	1.32	1.29	1.24
160 MeV Cl on Pd				
$E^* = 73.8$ MeV	$\langle I \rangle$ [$\hbar$]	37	42	46
$L_{\max} = 58\ \hbar$	$\langle T \rangle$	1.29	1.25	1.22

distributions it was assumed that the maximal angular momentum $L_{\max}$ is equal to that predicted by the model of Winther [10]. The average angular momentum of the calculated distributions as well as other reaction parameters are given in Table 1. These distributions were used as input to the statistical model code CASCADE.

Apart from the angular momentum distribution, an appropriate choice of the parameters describing the moment of inertia (hence the yrast line) has to be made. In the CASCADE code the moment of inertia is parametrized by three input values r_{eff}, δ and δ' as: $\Im = \Im_0(1 + \delta I^2 + \delta' I^4)$, with $\Im_0 = \frac{2}{5}A^{5/3}r_{\mathrm{eff}}^2$. In the present case, for the dominant residual nucleus ^{143}Eu the yrast spectroscopy is well known up to rather high spin values (55 $\hbar$). Therefore, the CASCADE input parameters $r_{\mathrm{eff}} = 0.97$ fm, $\delta = 1.43 \times 10^{-4}$ and $\delta' = -1.91 \times 10^{-8}$ were obtained from the fit of the rotational energy formula $E_{\mathrm{rot}} = \frac{\hbar^2}{2\Im} I(I+1)$ to the experimental data (see lower part of Fig. 2) and used as effective yrast line parameters in the calculations.

The choice of the parameters describing the yrast line and of the angular momentum distribution of the compound nucleus was verified by comparing the measured angular momentum dependence of the cross-section of the three main evaporation residues with those predicted by the statistical model. This comparison is shown in Fig. 3. It is

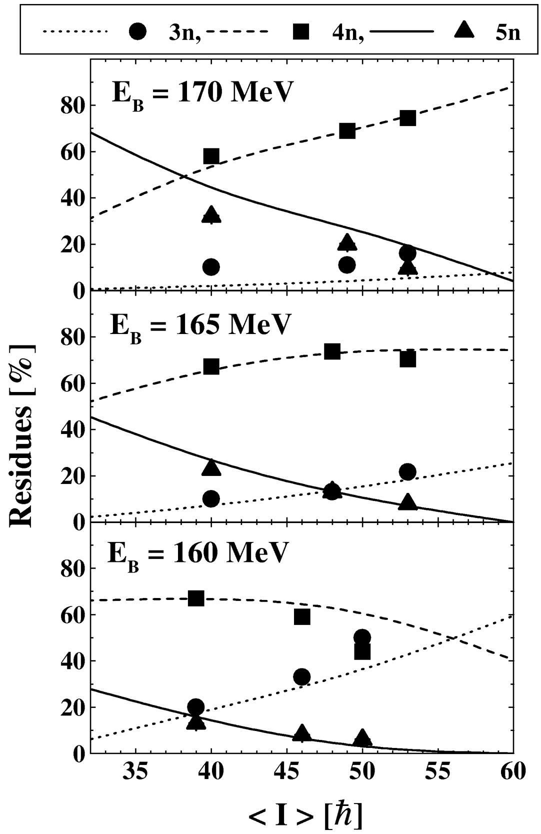

Fig. 3. Fraction of residue cross section as a function of spin obtained from lowest transitions in nuclei produced in reaction ^{37}Cl on ^{110}Pd for the beam energies 170 (top panel), 165 (middle panel) and 160 MeV (bottom panel). Only main residues were considered and the sum of their cross sections was normalised to 100%. Circles correspond to ^{144}Eu, squares to ^{143}Eu and triangles to ^{142}Eu. Lines show CASCADE calculations results.

Table 2
Cross sections of residual nuclei produced in 160 MeV Cl on Pd reaction

Residuum	Experimental data [19] (mb)	CASCADE calculations (mb)
^{139}Nd	≈ 0.5	0.5
^{140}Nd	< 0.5	0.2
^{139}Pm	6.3	4.9
^{140}Pm	6.1	4.2
^{141}Pm	1.9	1.0
^{143}Pm	≈ 0.1	0.07
^{141}Sm	3.7	4.6
^{142}Sm	9.8	9.3
^{143}Sm	$\geqslant 5.5$	6.2
^{144}Sm	0.5	0.7
^{141}Eu	3.5	4.9
^{142}Eu	22.0	21.7
^{143}Eu	33.0	33.5
^{144}Eu	7.2	6.9

particularly important to check the statistical model at this level since it was claimed [18] that in this mass region it is not possible to reproduce the residue distribution, unless very artificial input values (e.g., lowered bombarding energy) are used.

The measured cross-sections were obtained from the intensity of the low spin discrete γ-lines in the Ge-spectra gated by the folds corresponding to the average angular momentum of the decaying compound nucleus $\approx 39\ \hbar$, $\approx 48\ \hbar$ and $\approx 52\ \hbar$, respectively. As can be seen, the behaviour of the experimental data is satisfactorily reproduced by the calculations. Moreover, it has to be noticed that with this set of parameters the CASCADE calculations were able to reproduce (see Table 2) all the experimentally measured [19] cross-sections of the residual nuclei from the same reaction, giving additional confidence in the model.

The measured spectra of high-energy gamma rays obtained by gating on the three regions of folds are shown in Fig. 4. In this figure the data, presented with filled circles, are displayed together with the best fitting statistical model calculations (lines). In these calculations we assumed that the GDR strength function is described by a single Lorentzian function (three free parameters). The corresponding values of the fraction of the total energy weighted sum rule strength, of the centroid E_{GDR} and of the width Γ of the Lorentzian function are given in Table 3. The calculated spectrum was folded with the detector response function before its comparison with the experimental data.

For each fold region the average temperature of nuclear states on which the GDR is built was estimated from the CASCADE calculations as follows. The partial temperature T_i for each GDR decay step i at the excitation energy E_i was estimated as $T_i = \sqrt{(E_i^* - E_i^{\mathrm{rot}} - E_{\mathrm{GDR}})/a}$. In this expression for the level density parameter a the value $a = A/8\ \mathrm{MeV}^{-1}$ was used. The term E_{rot} represents the energy bound in the rotation which

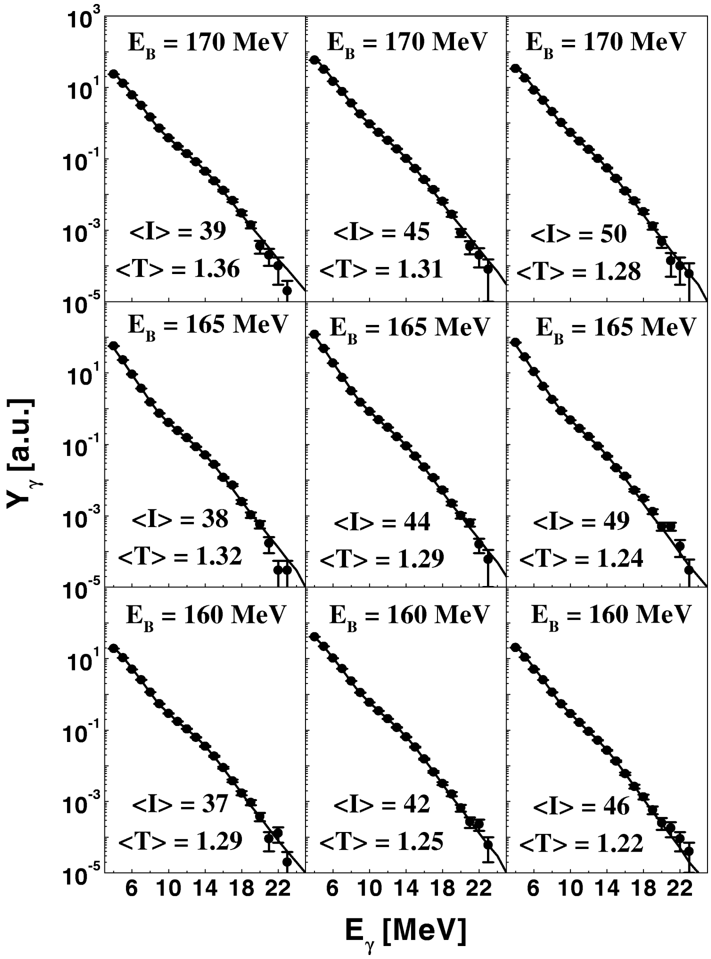

Fig. 4. Experimental high-energy γ-ray spectra (filled circles) for different beam energies and fold windows. Lines are the results from the fit of statistical model calculations.

was computed at the average angular momentum corresponding to the analysed fold. For the centroid energy of the giant dipole resonance the value $E_{\mathrm{GDR}} = 14.3$ MeV was used. The average temperature for the whole decay was defined as the weighted average of the partial temperatures $\langle T \rangle = \sum_i w_i T_i / \sum_i w_i$, where the weight w_i was obtained for each decay step i from the counts in the calculated spectrum at the γ-ray energy $E_\gamma = E_{\mathrm{GDR}}$. The average temperature deduced in this way is given in the legend of Fig. 4 and listed in the Table 1. An increase of the deduced values by ≈ 0.13 MeV is obtained, when one uses another approach (see, e.g., [20]), in which $\langle T \rangle = [d \ln(\rho)/dE]^{-1}$ is evaluated at $E = E_{\mathrm{CN}} - \langle E_{\mathrm{rot}} \rangle - E_{\mathrm{GDR}}$. As it can be seen, the differences between average temperatures of the analysed spectra (taken at different bombarding energy and angular momentum window) are quite small and most of the data points have an average temperature around 1.3 MeV.

Table 3
GDR parameters obtained from fit to the experimental data

E_{beam} (MeV)	$\langle I \rangle$ ($\hbar$)	S	E_{GDR} (MeV)	Γ (MeV)
170	39	0.91 ± 0.03	14.2 ± 0.1	8.8 ± 0.4
	45	0.98 ± 0.03	14.1 ± 0.1	8.9 ± 0.3
	50	1.01 ± 0.04	14.0 ± 0.1	8.8 ± 0.3
165	38	1.01 ± 0.03	14.2 ± 0.1	8.0 ± 0.2
	44	1.00 ± 0.02	14.3 ± 0.1	8.4 ± 0.2
	49	1.10 ± 0.03	14.2 ± 0.1	8.6 ± 0.3
160	37	0.83 ± 0.02	14.3 ± 0.1	8.0 ± 0.2
	42	0.88 ± 0.02	14.3 ± 0.1	8.4 ± 0.2
	46	0.86 ± 0.03	14.2 ± 0.1	8.7 ± 0.4

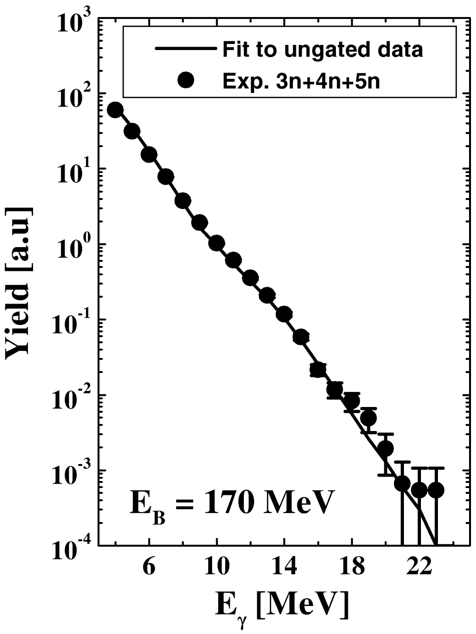

Fig. 5. Experimental high energy spectrum gated by discrete transitions in ^{142,143,144}Eu (filled circles) compared with calculations (solid line) performed using CASCADE. The calculated spectrum, normalised at 6 MeV to the experimental points, was obtained by a fit to the total (not gated by discrete transitions) experimental spectra.

The high-energy γ-ray spectrum gated by the most intense discrete γ transitions among the levels of the main residual nuclei (^{144,143,142}Eu) is shown in Fig. 5. In order to see whether or not the less exclusive spectrum, namely that gated only by high fold in the multiplicity filter, contains contributions from non-fusion reactions we compared the best fitting calculations shown in Fig. 4 with the high-energy γ-ray spectrum gated by the discrete low lying transitions in the three main evaporation channels. The two spectra are almost identical in the energy range 5–15 MeV, where the eventual non-fusion contributions are expected. This comparison indicates that the gate on fold is indeed adequate to select the compound nucleus process.

In order to display spectra on a linear scale to emphasise the GDR region, the experimental spectra were converted to our best estimate of the photon absorption cross section (GDR strength function), represented by the quantity $F_{1L}(E_\gamma) * Y_\gamma^{\exp}(E_\gamma)/Y_\gamma^{\mathrm{cal}}(E_\gamma)$. In this formula $Y_\gamma^{\exp}(E_\gamma)$ is the experimental spectrum and $Y_\gamma^{\mathrm{cal}}(E_\gamma)$ — the calculated spec-

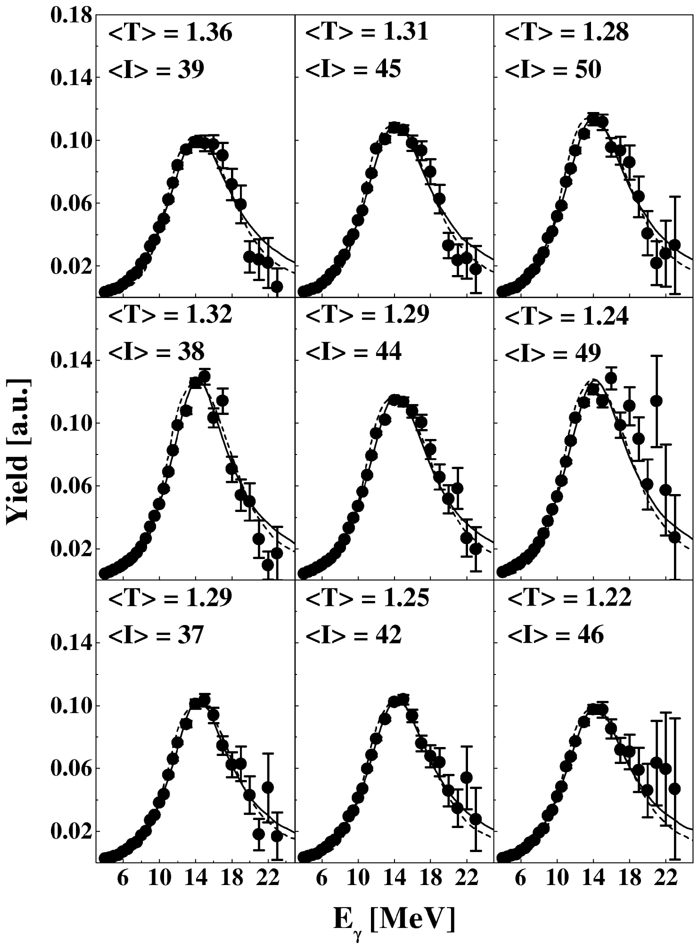

Fig. 6. GDR strength functions (filled circles) obtained from experimental data (see Fig. 4) as a quantity $F_{1L}(\gamma)Y_{\exp}(\gamma)/Y_{\mathrm{fit}}(\gamma)$. $Y_{\exp}(\gamma)$ is the experimental spectrum and $Y_{\mathrm{fit}}(\gamma)$ is the calculated spectrum with the best-fit GDR parameters which were put into the single Lorentzian function $F_L(\gamma)$ plotted in full drawn lines. Dashed lines are the strength functions calculated by the thermal fluctuation model. In the top panel, data for 170 MeV are presented, middle panel for 165 MeV, bottom 160 MeV. The average spin and temperature of the nucleus (on which the GDR is built) are written in the figure's legend.

trum assuming that the GDR decay can be represented by the single Lorentzian function $F_{1L}(E_\gamma)$, being the best fit to the experimental spectrum.

The experimental data (points) and the Lorentzian functions $F_{1L}(E_\gamma)$ used in the calculations (solid lines) are shown in Fig. 6. A good overall agreement between experimental points and the fit is found for all the cases, although some details of the line shape are not reproduced by the single Lorentzian GDR function. In the same figure the results of the model calculations discussed in the following section are also shown with dashed lines.

An attempt to fit the experimental spectra with the double Lorentzian GDR function (i.e., six free parameters) has been made, and the resulting spectra, again converted to the absorption functions, are displayed in Fig. 7. The parameters (strength, centroid and the

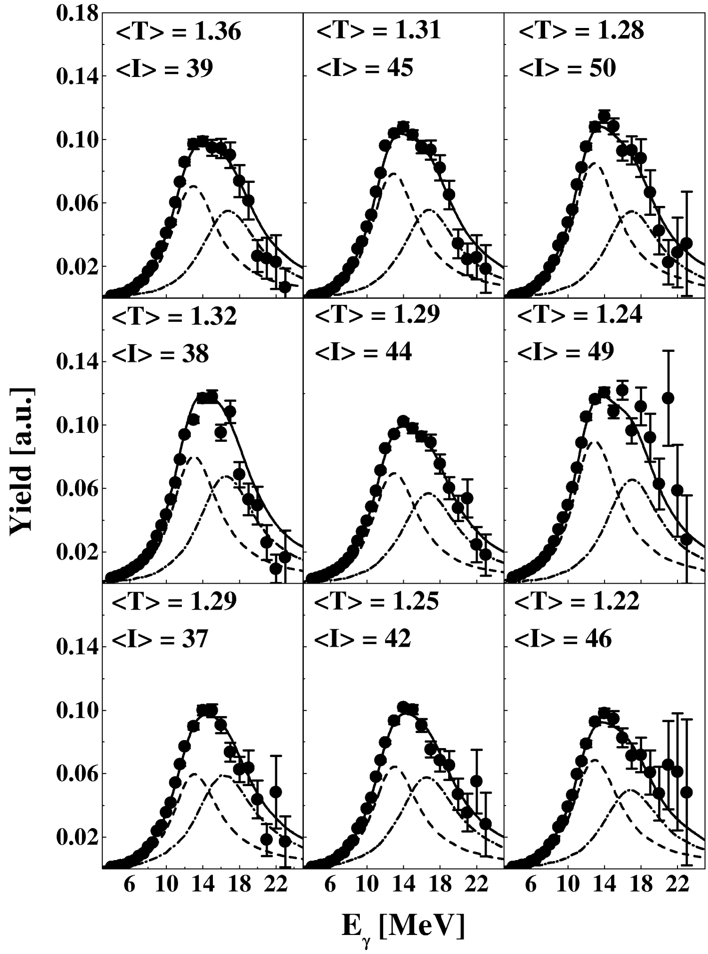

Fig. 7. As in Fig. 6, but the plotted quantity is $F_{2L}(\gamma)Y_{\mathrm{exp}}(\gamma)/Y_{\mathrm{fit}}(\gamma)$, where $Y_{\mathrm{fit}}(\gamma)$ is the best fitted calculated spectrum using double Lorentzian for the GDR decay. $F_{2L}(\gamma)$, drawn in solid line, is the sum of two Lorentzian functions (dashed lines) corresponding to two components of the GDR.

Table 4
Parameters of the two fitted GDR components

E_{beam} (MeV)	$\langle I \rangle$ ($\hbar$)	S	E_{GDR} (MeV)	Γ (MeV)	β
170	39	0.43 ± 0.02	12.9 ± 0.1	5.9 ± 0.1	
		0.41 ± 0.03	16.8 ± 0.1	7.3 ± 0.4	0.29 ± 0.01
	45	0.48 ± 0.02	12.9 ± 0.1	5.9 ± 0.1	
		0.40 ± 0.03	16.8 ± 0.1	7.0 ± 0.3	0.29 ± 0.01
	50	0.52 ± 0.02	12.9 ± 0.1	5.9 ± 0.1	
		0.40 ± 0.04	17.0 ± 0.2	7.2 ± 0.5	0.30 ± 0.02
165	38	0.49 ± 0.02	13.0 ± 0.1	5.9 ± 0.1	
		0.51 ± 0.03	16.5 ± 0.1	7.3 ± 0.3	0.26 ± 0.01
	44	0.42 ± 0.02	13.0 ± 0.1	5.8 ± 0.1	
		0.43 ± 0.02	16.7 ± 0.1	7.4 ± 0.2	0.27 ± 0.01
	49	0.54 ± 0.02	12.9 ± 0.1	5.8 ± 0.1	
		0.48 ± 0.03	17.0 ± 0.1	7.1 ± 0.4	0.30 ± 0.01
160	37	0.36 ± 0.02	13.1 ± 0.1	5.8 ± 0.1	
		0.46 ± 0.03	16.4 ± 0.1	7.7 ± 0.3	0.24 ± 0.01
	42	0.39 ± 0.02	13.0 ± 0.1	5.9 ± 0.1	
		0.45 ± 0.03	16.6 ± 0.1	7.7 ± 0.2	0.27 ± 0.01
	46	0.42 ± 0.02	12.9 ± 0.1	5.9 ± 0.1	
		0.38 ± 0.04	16.8 ± 0.2	7.5 ± 0.5	0.29 ± 0.02

width of each GDR component) corresponding to this fit are given in Table 4. One can note that the values of the strength of the 2 fitted components are very similar. This indicates that the effective shape is neither purely oblate nor prolate, but rather is a mixture of different shapes including possibly also the non-axially symmetric ones. This is consistent with the predictions of the thermal shape fluctuation model, discussed in the next section. From the values of the centroids of the two best fitting Lorentzian components the value of the effective quadrupole deformation parameter β was deduced. In particular the expression $\beta \approx 1.06\frac{E_2-E_1}{E_{\text{GDR}}}$ was employed, in which E_1 and E_2 are the centroid energies of the Lorentzian functions and E_{GDR} is the GDR centroid energy for the spherical case. The corresponding values are reported in Table 3.

4. Experimental results and comparison with theory

The measured angular momentum dependence of the GDR width obtained from single Lorentzian fits (see Table 3) is displayed in the upper part of Fig. 8. In the figure one can see a smooth systematic increase of the GDR width from $\Gamma_{\text{GDR}} \approx 8$ MeV at $\langle I \rangle = 37\ \hbar$ to $\Gamma_{\text{GDR}} \approx 8.8$ MeV at $\langle I \rangle = 50\ \hbar$. Only the width measured at $\langle I \rangle = 39\ \hbar$ for $E_B = 170$ MeV deviates from the general trend, but this could be due to the higher average temperature ($\langle T \rangle = 1.4$ MeV) of this point as compared to that the other points. The measured experimental behaviour is expected to reflect the role of the quadrupole

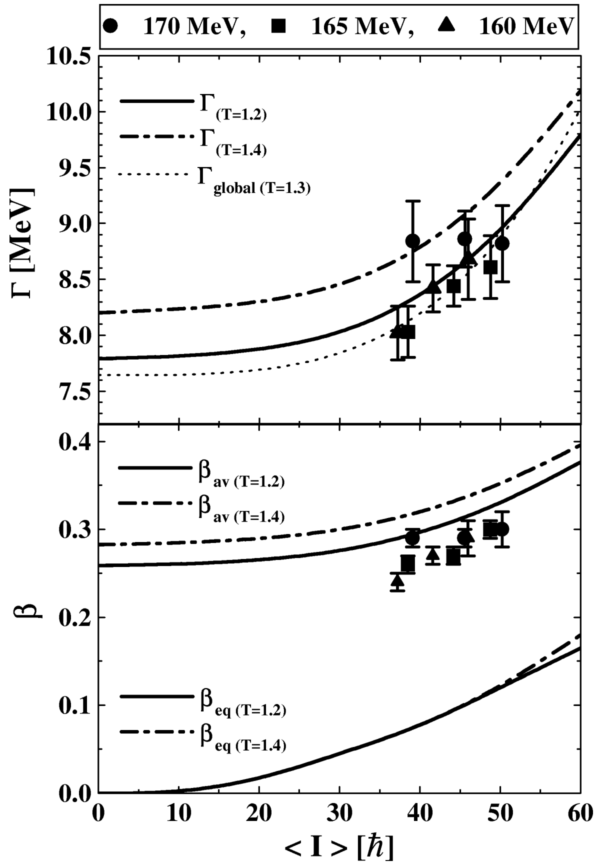

Fig. 8. Measured GDR widths obtained from the single Lorentzian fits (top panel) and deformation parameters β deduced from the splitting of the GDR components (bottom panel) plotted as a function of angular momentum in comparison with thermal shape fluctuation predictions for $T = 1.2$ MeV (solid line) and $T = 1.4$ MeV (dot-dashed line). The points correspond to the experimental data obtained for different beam energies: circles show the data from reaction with 170 MeV beam energy, squares — with 165 MeV and triangles — with 160 MeV. In the bottom panel the solid and dashed lines show the calculated equilibrium β_{eq} and average β_{av} deformation parameters for $\langle T \rangle = 1.2$ and 1.4 MeV. The GDR width calculated with the phenomenological formula obtained from the fit to the global data is shown as thin dotted line in the top panel.

deformation on the GDR width and line-shape. According to the model of thermal shape fluctuations [21,22] the GDR line-shape mirrors the quadrupole deformation as it consists on the superposition of three Lorentians whose centroids are inversely proportional to the nuclear principal axis. The details of the model are reported in Refs. [4,21]. Here we recall some of the basic expressions and assumptions which were used to predict the line shapes and their corresponding widths reported in present paper. As temperature induces large fluctuations in nuclear deformation and orientation a broad ensemble of shapes would contribute to the GDR line-shape and width. The higher the temperature, the broader the ensemble. The probability to have a hot rotating nucleus, at temperature T and spin I, with a definite nuclear quadrupole shape (parameterised by the Hill–Weeler parameters β and γ) and orientation (defined by the use of the three Euler angles ψ, θ, and ϕ relative to an external reference frame) is governed by the Boltzman factor:

$$P(\beta,\gamma,\phi,\theta,\psi;T,I) \propto \exp\left[\frac{-F}{T}\right], \tag{1}$$

where the nuclear free energy F is a function of the deformation parameters, Euler angles, angular momentum, and temperature of the compound nucleus. In the adiabatic assumption, assuming that the time scale associated to thermal shape and orientation fluctuations is long compared to the time necessary to the GDR oscillation to couple with the quadrupole nuclear shape, the GDR line-shape is a weighted average over all the possible shapes and orientations:

$$\sigma(E) = Z_J^{-1}\int \frac{\mathcal{D}[\alpha]}{\mathcal{I}(\beta,\gamma,\theta,\psi)^{3/2}}\,\sigma(\alpha,\omega_J;E)\,\mathrm{e}^{-F(T,\alpha,J)/T}, \tag{2}$$

where α denotes the deformation and orientation parameters, E is the photon energy, $\mathcal{D}[\alpha] = \beta^4\,d\beta\,\sin(3\gamma)\,d\gamma\,\sin\theta\,d\theta\,d\phi\,d\psi$ is the volume element, $Z_J = \int \mathcal{D}[\alpha]/\mathcal{I}^{3/2}\,\mathrm{e}^{-F/T}$. For the quantity $\mathcal{I}$ the expression

$$\mathcal{I}(\beta,\gamma,\theta,\psi) = I_1\cos^2\psi\sin^2\theta + I_2\sin^2\psi\sin^2\theta + I_3\cos^2\theta, \tag{3}$$

was used where the I_k represent the deformation-dependent principal moments of inertia. The free energy has been evaluated in the cranking approximation as described in [4,21]. For the expression of $\sigma(\alpha,\omega_J;E)$ a superposition of three Lorentzian function was used. This is because the GDR in a nucleus consists of three fundamental modes corresponding to vibrations along each of the intrinsic axes k with a centroid energy E_k given by the Hill–Wheeler formula [21], and an intrinsic damping width of $\Gamma_k = \Gamma_0^{\downarrow}(E_k/E_{\mathrm{GDR}})^{\delta}$, where, for ^{147}Eu, the values $E_{\mathrm{GDR}} = 14.3$ MeV, $\Gamma_0^{\downarrow} = 4.5$ MeV, and $\delta = 1.9$ were used.

The calculations of the spin dependence of the GDR width in the studied ^{147}Eu are shown in the upper part of Fig. 8 as a solid ($T = 1.2$ MeV) and dashed ($T = 1.4$ MeV) lines. It is evident that the data are well described by the model. In a similar way it is possible to calculate the spin dependence of the equilibrium deformation β_{eq} (defined as the most probable deformation) and the average deformation β_{av} defined as a Boltzmann weighted average,

$$\beta_{\mathrm{av}} = Z^{-1}\int \frac{\mathcal{D}[\alpha]}{\mathcal{I}^{3/2}}\,\beta\exp(-F/T). \tag{4}$$

Both deformations, plotted in the bottom part of Fig. 8, show very different behaviours. The equilibrium deformation β_{eq} (which is expected to be controlled by the centrifugal force) is small and shows a definite increase with angular momentum. The average deformation β_{av} is larger, constant at lower angular momenta and rather weakly increasing at high angular momenta. The solid points in the plot correspond to deformation parameters β deduced from the experiment, as obtained from the double Lorentzian analysis (see Table 4). The angular momentum dependence of the experimental points representing the deformation parameter is found, similarly as for the GDR width, to be in good agreement with the predicted dependence of the average shapes corresponding to a temperature $T = 1.2$ MeV. This agreement gives a stronger support to the thermal fluctuation model which predicts well both the width of the GDR strength function if a single Lorentzian analysis is made and the average deformation if a two Lorentzian components analysis is made.

Also the analogy of the dependence of the GDR width and of the quadrupole deformation parameter on angular momentum supports the basic assumption of the thermal fluctuation model, namely that the increase of the GDR width with angular momentum reflects the increase in the splitting of the GDR components due to the increase of the nuclear deformation induced by the fast rotation.

Fig. 8 shows furthermore that although the fluctuation calculation for $T = 1.2$ MeV reproduce the experimental GDR width, the same calculation seem to overpredict the experimental deformation parameters inferred from the fitted 2-Lorentzian splittings. This can be explained by the fact, that the calculated average deformation is related to the width of the strength distribution, which results both from a broadening of the Lorentzian components as well as a possible splitting. Thus the deformation inferred from the splitting alone must lie in between the equilibrium deformation and the average deformation (see [23]).

In addition to the results from the thermal shape fluctuations model, in the upper part of Fig. 8 is drawn (as a dotted line) the GDR width calculated using the phenomenological global formula of [24,25]. The parameters of this formula were obtained by a fit to all known values of GDR widths over the whole nuclear chart, at different temperatures and angular momenta. The dotted line of Fig. 8 shows the value of the GDR width in the case of the Eu nucleus at temperature $T = 1.3$ MeV. As can be seen, the phenomenological formula gives in the present case a very good description of both the more exact calculations and the data.

It is also important to notice that the present spectra do not show any trace of superdeformation that have been found near the yrast line in the residual nucleus ^{143}Eu. This is consistent with the analysis of more exclusive spectra which indeed indicates that the superdeformation is a property that this nucleus has only around the yrast line ($U <$ 15 MeV) and that therefore cannot be seen in more inclusive spectra like the present ones which are dominated by the decay of the hot compound nucleus.

In order to compare the behaviour of the GDR width as a function of spin in different mass regions, the present results are displayed in Fig. 9 together with the data for Sn, W, and Hg nuclei [4–6] all obtained using set-ups including a multiplicity filter. For the sake of clarity only the Eu data at constant $\langle T \rangle = 1.3$ MeV and with different values of the angular momentum are shown in the figure. The results of the calculations made using the thermal shape fluctuations model are also plotted in the same figure. The Eu data show a weak angular momentum dependence, much weaker than the one of Sn but stronger than those of heavier nuclei W and Hg. As far as the comparison to the theoretical model is concerned, one can notice that in general the agreement with the experiment is rather good in spite of some deviations in the case of Sn at the highest angular momentum values.

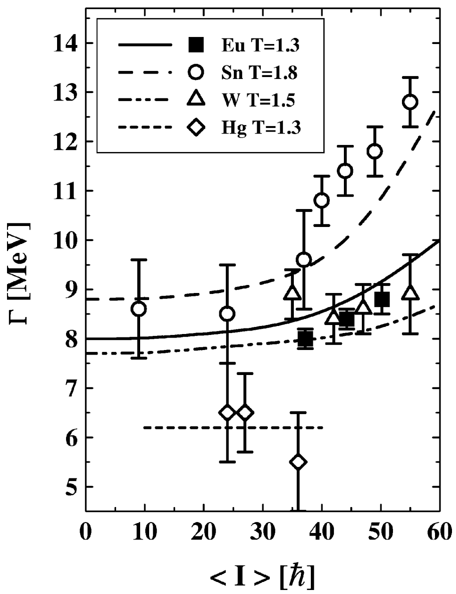

Fig. 9. GDR widths measured in several experiments [4–6] as a function of angular momentum compared with calculations. The solid squares are the present results for ^{147}Eu at the average temperature $\langle T \rangle = 1.3$ MeV, while the open symbols are results from previous works. The lines show the results from corresponding calculations with the thermal shape fluctuations model.

5. Summary and conclusions

The giant dipole resonance in the excited ^{147}Eu nucleus has been studied in the angular momentum interval from 35 to 50 $\hbar$ and at temperatures of 1.2–1.4 MeV. At variance from most previous studies, both the high-energy and low-energy γ-ray spectra were measured and analysed with the statistical model. This provided more complete test for the statistical γ-decay of compound nuclei, which is the basic assumption of all GDR studies at finite temperature.

The GDR width was found to have a weak dependence on angular momentum, a behaviour intermediate between that found for the Sn and Hg nuclei. This is well understood by the model of thermal shape fluctuation, pointing that the main damping mechanism effect is related to nuclear shape effects. The effective nuclear deformation was also obtained from the experimental data. In particular the value of the quadrupole deformation was deduced and compared with the model predictions. The findings are very similar to the predicted values of the average deformation and distinctively different from the equilibrium deformation. This result supports the basic assumption of the thermal fluctuation model, namely that the dipole vibration is not only coupled to the most probable deformation but to the ensemble of the nuclear deformations characterising the nucleus at finite temperature and angular momentum. In addition, also in this case was found the evidence that the collisional damping width is basically equal to that measured at temperature $T = 0$.

To complete the study of the GDR built on excited states in this mass region it would be desirable to have also angular distribution measurements which can provide an even more stringent test of the thermal shape fluctuation model, being dependent also on orientation fluctuations.

Acknowledgements

The authors wish to thank M. Kicińska-Habior and D. Kusnezov for very helpful discussions. Financial support from the Polish State Committee for Scientific Research (KBN Grant No. 2 P03B 001 16), from the Danish Natural Science Research Council and from INFN, Italy is gratefully acknowledged. This work was carried out in part under the auspices of the U.S. Department of Energy by Lawrence Livermore National Laboratory under contract No. W-7405-ENG-48.

References

[1] A. Bracco, P.F. Bortignon, Nucl. Phys. A 649 (1999), Proceedings of the Topical Conference on Giant Resonances, in particular see D.M Brink, 218c.
[2] P.F. Bortignon, A. Bracco, R.A. Broglia, Giant Resonances: Nuclear Structure at Finite Temperature, Gordon Breach, New York, 1998.
[3] A. Bracco, F. Camera, M. Mattiuzzi, B. Million, M. Pignanelli, J.J. Gaardhøje, A. Maj, T. Ramsøy, T. Tveter, Z. Żelazny, Phys. Rev. Lett. 74 (1995) 3748.
[4] M. Mattiuzzi, A. Bracco, F. Camera, W.E. Ormand, J.J. Gaardhøje, A. Maj, B. Million, M. Pignanelli, T. Tveter, Nucl. Phys. A 612 (1997) 262.
[5] E. Ramakrishnan, T. Baumann, A. Azhari, R.A. Kryger, R. Pfaff, M. Thoennessen, S. Yokoyama, J.R. Beene, M.L. Halbert, P.E. Mueller, D.W. Stracener, R.L. Varner, R.J. Charity, J.F. Dempsey, D.G. Sarantites, L.G. Sobotka, Phys Rev. Lett. 76 (1996) 2025.
[6] F. Camera, A. Bracco, S. Leoni, B. Million, M. Mattiuzzi, M. Pignanelli, A. Maj, M. Kmiecik, R. Bark, J. Bearden, J.J. Gaardhøje, W.E. Ormand, T. Lonnroth, R. Osterbacka, Phys. Rev. C 60 (1999) 014306.
[7] F. Camera, A. Bracco, A. Maj, B. Herskind, A. Atac, P. Bosetti, R. Bark, I.G. Bearden, J.J. Gaardhøje, M. Kmiecik, S. Leoni, M. Mattiuzzi, G. Turri, Eur. Phys. J. A 2 (1998) 1.
[8] A. Bracco, F. Camera, S. Frattini, S. Leoni, B. Million, A. Maj, M. Kmiecik, B. Herskind, M. Bergström, Acta. Phys. Pol. B 30 (1999) 501.
[9] A. Bracco, F. Camera, S. Leoni, B. Million, S. Frattini, A. Maj, B. Herskind, A. Algora, A. Axelsson, M. Bergström, N. Blasi, M. Castoldi, A. Gadea, M. Kmiecik, G. Lo Bianco, J. Nyberg, M. Pignanelli, J. Styczeń, M. Zięblińksi, A. Zucchiatti, Physica Scripta, in print.
[10] A. Winther, Nucl. Phys. A 594 (1995) 203.
[11] A. Maj, J.J. Gaardhøje, A. Atac, S. Mitarai, J. Nyberg, A. Virtanen, A. Bracco, F. Camera, B. Million, M. Pignanelli, Nucl. Phys. A 571 (1994) 185–220.
[12] B. Herskind, Nucl. Phys. A 447 (1985) 395.
[13] G. Sletten, J. Gascon, J. Nyberg, in: Proc. Int. Conf. on Spectroscopy of Heavy Nuclei, Crete, Greece, Int. Phys. Ser., Vol. 105, 1989.
[14] F. Pühlhofer, Nucl. Phys. A 280 (1977) 267.
[15] W. Reisdorf, Z. Phys. A 300 (1997) 227.
[16] M. Kicińska-Habior, K.A. Snover, C.A. Gossett, J.A. Behr, G. Feldman, H.K. Glatzel, J.H. Gundlach, E.F. Garman, Phys. Rev. C 36 (1987) 612.

[17] M. Kicińska-Habior, private communication.
[18] L.H. Zhu, M. Cinausero, S. Lunardi, G. Viesti, D. Bazzacco, G. De Angelis, M. De Poli, D. Fabris, E. Fioretto, A. Gadea, F. Lucarelli, M. Lunardon, N.H. Medina, D.R. Napoli, C.M. Petrache, G. Prete, C. Rossi Alvarez, Nucl. Phys. A 635 (1998) 325.
[19] M. Piiparinen, A. Atac, J. Blomqvist, G.B. Hagemann, B. Herskind, R. Julin, S. Juutinen, A. Lampinen, J. Nyberg, G. Sletten, P. Tikkanen, S. Törmänen, A. Virtanen, R. Wyss, Nucl. Phys. A 605 (1996) 191, and references therein.
[20] M.P. Kelly, K.A. Snover, J.P.S. van Schagen, M. Kicińska-Habior, Z. Trznadel, Phys. Rev. Lett. 82 (1999) 3404.
[21] W.E. Ormand, P.F. Bortignon, R.A. Broglia, Nucl. Phys. A 618 (1997) 20.
[22] Y. Alhassid, N. Whelan, Nucl. Phys. A 565 (1993) 427.
[23] J.H. Gundlach, K.A. Snover, J.A. Behr, C.A. Gosset, M. Kicińska-Habior, K.T. Lesko, Phys. Rev. Lett. 65 (1990) 2523.
[24] D. Kusnezov, Y. Alhassid, K.A. Snover, Phys. Rev. Lett. 81 (1998) 542.
[25] D. Kusnezow, private communication.